Solar Equator EUV Intensity Fluctuation during 2016 Sep 6 NOAA Active Region 12585 Arcing

George Tremberger, Sunil Dehipawala, M. Chantale Damas,
Raul Armendariz, and Tak Cheung

Physics Department, Queensborough Community College/ City University of New York, USA

Abstract: *The Solar Dynamics Observatory EUV 9.4 nm data was used to study the intensity fluctuation at the solar equator during the Sep 6 2016 NOAA Active Region (AR) 12585 Arcing. The 9.4 nm intensity data parallel with the solar equator showed correlation with the adjacent image row-data (R-sq >0.95) for the studied region near AR 12585. The analysis of the percent increment in the intensity data series (parallel with the solar equator) showed that the fractal dimension values (>2.05) of the studied series correlated with standard deviations. The interpretation of the percent increment in the intensity as a Gaussian-like probability density function via a Fokker-Plank equation model is discussed.*
Keywords: *Fokker-Planck equation model, Intensity fluctuation, SDO/AIA 9.4 nm data, Percent increment data series, Solar Active Region.*

I.   Introduction

The Solar Dynamics Observatory EUV 9.4 nm data was used to study the solar equator intensity fluctuation during the 2016 Sep 6 NOAA Active Region 12585 Arcing. The 9.4 nm contains mostly the Fe XVIII emission data with small amounts from the 19.3 nm and 17.1 nm channels [1]. The AR 12585 event was first labeled by NOAA on Sep 1 (Figure 1). On Sep 6 the AR 12585 had moved onto the central region of the solar disk.
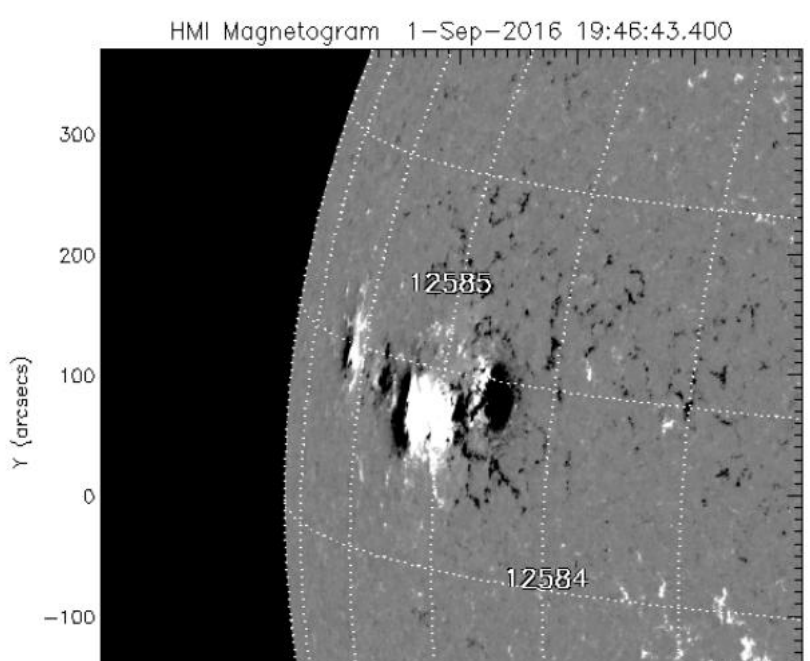

Figure 1: NOAA AR 12585 illustration. (https://www.solarmonitor.org/)

II.   Data And Methods

The Solar Dynamics Observatory AIA/HMI data are available from the NASA SDO website. The FITS data are available from http://jsoc.stanford.edu/data/aia/synoptic/2016/09/. The SDO/AIA 9.4 nm FITS image data on Sep 6 UT1200 is shown in Figure 2. When an observed intensity Int1 was adjacent to another intensity Int2 parallel with the solar equator, the intensity percent increment could be calculated as (Int2 – Int1)/Int1. The fractal dimension values for the intensity percent increment data series were calculated using the Higuchi algorithm, which have been described by us in an earlier publication on an open access platform [2].
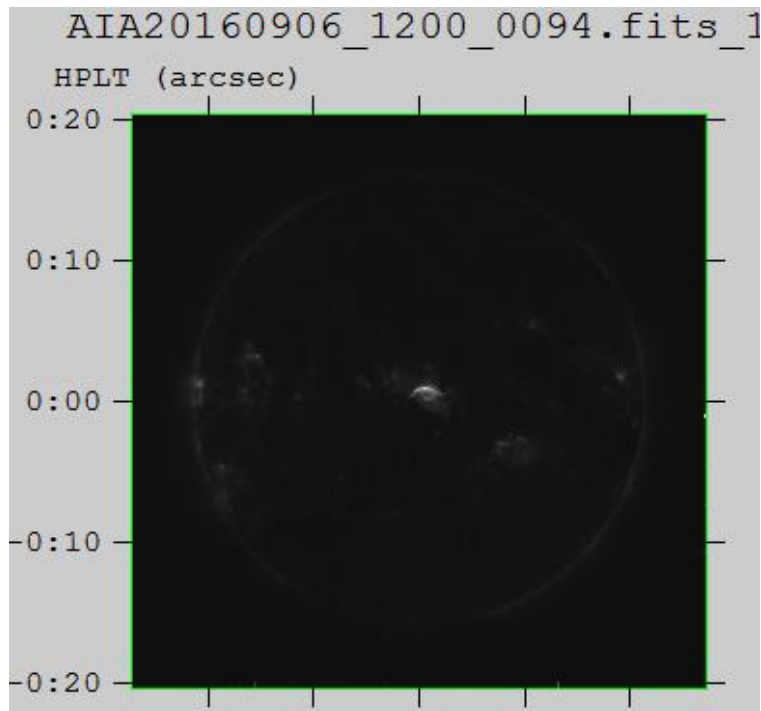
Figure 2: NOAA AR 12585 on 2016 Sep 6 UT1200. The intense arcing is visible in the image. Whether the arc exhibited symmetry like an arch was not investigated in this project. The NASA Fv Image Viewer was used to read the 1024 by 1024 bits SDO/AIA 9.4 nm FITS image. The highest intensity of about 147 DN/sec was observed at row number 532 and 519 pixel location. The solar equator was taken as row number 512.

III.   Results Of Image Data Analysis

The SDO/AIA 9.4 nm FITS image data in Figure 2 were analyzed. The intensity at row-number 512 across the image is shown in Figure 3. .
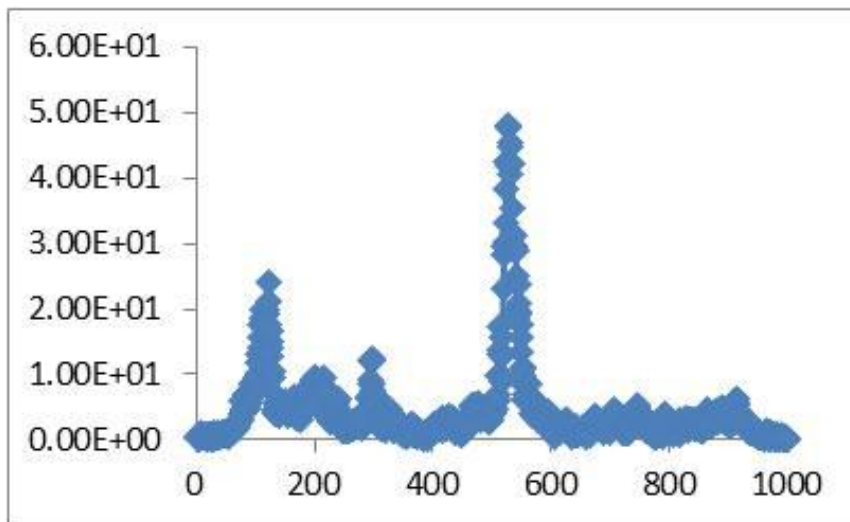

Figure 3: The intensity versus pixel number across the Figure 2 image at the center (row number 512). The pixels from number 125 to 900 would lie within the solar disk.

The result of a correlation analysis on the region between the 385th pixel to 650th pixel for 512-row intensity and 511-row intensity is shown in Figure 4. A similar high correlation, R-sq > 0.93 on the region between 125th pixel to pixel 384th pixel for 512-row intensity and 511-row intensity was observed. However a correlation of R-sq = 0.66 on the region between 641st pixel to pixel 900th pixel for 512-row intensity and 511-row intensity was observed. The correlation was observed to drop slightly as the distance to the 512-row

increased and further away from the AR 12585. For example, the correlation would drop to R-sq = 0.75 between 512-row and 510-row data on the region from the 385th pixel to 650th pixel.
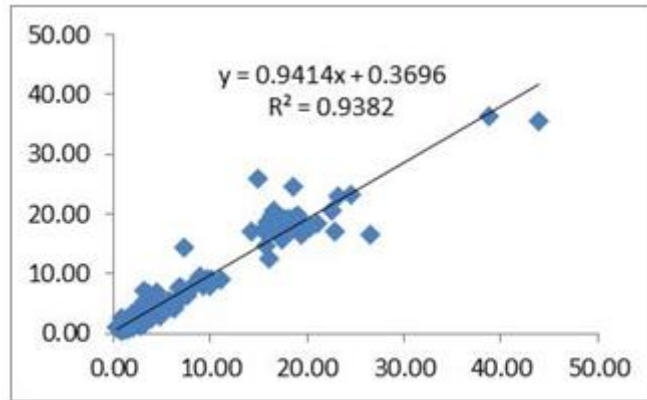

Figure 4: The correlation of intensity for the Figure 3 data at row-number 512 with its adjacent row at row-number 511. The analyzed region was between the 385th pixel to 650th pixel. The row number definition in the NASA Fv Image Viewer was used.

The intensity percent increment series analysis results for the fractal dimension values are shown in Figure 5. The region between the 385th pixel to 650th pixel was analyzed.
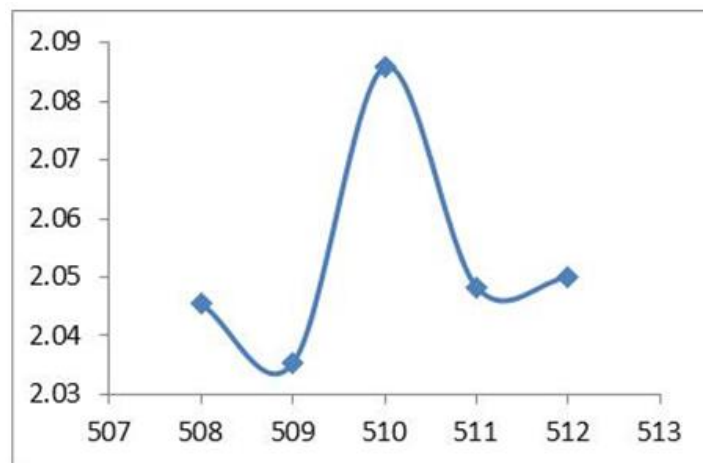

Figure 5: The fractal dimension y-axis versus row-number. The row number definition in the NASA Fv Image Viewer was used.

The corresponding intensity percent increment series analysis results for the histogram standard deviations and averages are shown in Figure 6.
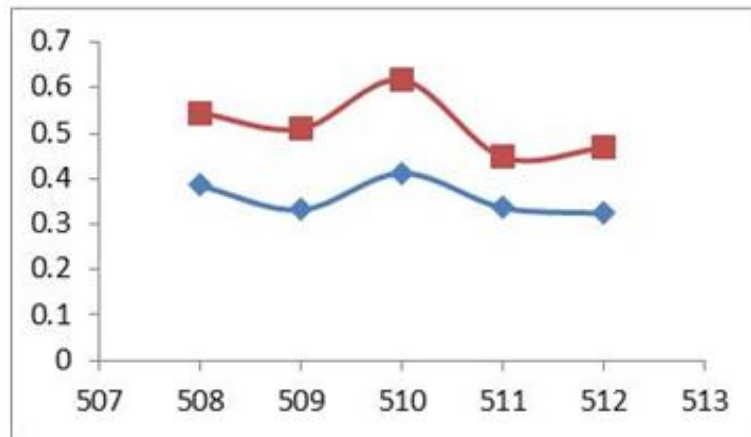
Figure 6: The histogram standard deviation y-axis versus row-number x-axis, upper curve. The histogram average*10 y-axis versus row-number x-axis, lower curve; the row number definition in the NASA Fv Image Viewer was used.

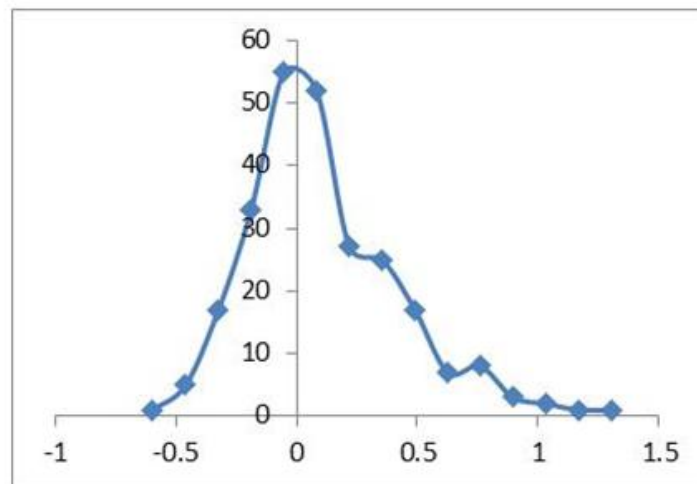The histogram of 512-row intensity percent increment series is shown in Figure 7.

Figure 7: The histogram of 512-row intensity percent increment series. The row number definition in the NASA Fv Image Viewer was used.

IV.   Discussion

The high correlation (R-sq = 0.94) of the intensity data in the studied mid region (385th pixel to 640th pixel) illustrated in Figure 4 and the relatively low correlation (R = 0.66) for the studied 641st pixel to 900th pixel region would be consistent with a scenario where the equatorial magnetic lines are being entangled with interaction driven by the solar rotational motion. Another general interpretation would be an anisotropy related mechanism such that regions near AR 12585 would have different correlations [3]. Fractal dimension analysis for correlated randomness in the percent increment data fluctuation, illustrated in Figure 5, revealed fractal dimension values larger than the theoretical value of 2 for a random series.   Frequency simulation on the expected fractal dimension values for a group of computer- generated random sequences showed that the 2.0 fractal dimension value frequency would be about double in comparison to the 2.05 fractal dimension value frequency. Such correlated randomness study on SDO/AIA data via fractal dimension analysis has also been published by others [4]. On the other hand, the intensity percent increment series could be analyzed using the probability density function concept, illustrated in Figure 7 as a histogram.   The fractal dimension values illustrated in Figure 5 were found to correlate mildly with the standard deviation values illustrated in Figure 6 (R-sq = 0.57, N = 5). The Fokker-Planck equation usually describes the evolution of a probability density function in time. The spatial evolution of the histogram parameters, standard deviation and average values illustrated in Figure 6, could be described by a Fokker-Planck equation model. The usual Fokker-Planck equation for describing time evolution of probability density function, $\partial f/\partial t = (\sigma 2 /2) * \partial(\partial f/\partial I)/\partial I) + \mu * \partial f/\partial I$, could be replaced with a spatial variable with a unique direction as the distance increases from the active region

in this project [5, 6]. This replacement is consistent with a recent study which found that time as a variable can be modeled as the de- coherence of a physical entity such as a wavefunction [7], and that our correlation study result, illustrated in Figure 4, would support a de- coherence concept related to a distance increase from the active region. Note that the spatial vertical distance variable in the above proposed Fokker-Planck equation model is different from the horizontal distance variable used to calculate the intensity percent increment series. The spatial vertical distance variable x in Figure 8 would correspond to the row-number variable in the NASA Fv Image Viewer definition.

Fokker-Planck equation

$$\partial f / \partial x = (\sigma^2 / 2) * \partial(\partial f / \partial I)/\partial I + \mu * \partial f / \partial I$$

Figure 8: Fokker Planck equation tracks the development of the intensity probability density function $f(I, x)$ with I_0 for the initial intensity value and x_0 as the initial spatial value. The right hand side contains the diffusion term with coefficient $\sigma(I_0, x_0)$, and the advection term with coefficient $\mu(I_0, x_0)$.

The histogram shown in Figure 7 could be decomposed into two Gaussian-like sub-histograms as displayed in Figure 9. In general, when the percent increment data series of a random variable behaves like a Gaussian distribution, the random variable would follow a log-normal distribution because $d(\log(x)) = dx/x$. Therefore the analysis would suggest that the intensity variable would have a log-normal distribution with an origin being related to the multiplicative product of two or more Gaussian variables. The proposed methodology in this report could shed light on the Sun's effect on Earth Station cosmic ray detection [8] and spacecraft sky survey studies [9], as well as the possible effect of planetary tides on the Sun [10]. Last but not least, the proposed methodology could also serve as an educational platform for undergraduate students to study space weather projects with online open access educational information and SDO/AIA/HMI intensity data [11, 12].
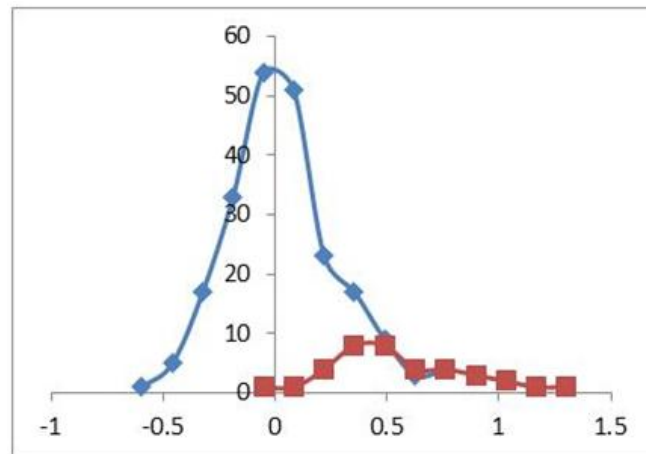

Figure 9: The two sub-histograms of the histogram in Figure 7.

V. Conclusion

The project results showed that the 2016 Sep 6 SDO EUV 9.4 nm intensity percent increment data in the studied regions near AR 12585 contain correlations that would be consistent with a model of solar rotation related magnetic interaction. Fractal dimension analysis results also supported the presence of correlated randomness in the percent increment data fluctuation. The interpretation of the intensity percent increment as a probability intensity function via a Fokker-Planck equation model would support a log-normal distribution for the intensity variable in the studied regions. Applications could include similar analyses of other SDO/AIA data, studies of solar rotation effect on magnetic line entanglement via multifractal analysis, etc.

Acknowledgements

References

[1] Ignacio Ugarte-Urra and Harry P. Warren, Determining heating time scales in solar active region cores from AIA/SDO Fe XVIII images. *arXiv:1311.6346v1 (2012)*. http://lanl.arxiv.org/abs/1311.6346112-116.

[2] George Tremberger, Sunil Dehipawala, Raul Amendariz, Chantale Damas and Tak Cheung, Cosmic Ray time series data fractal analyses during Solar AR 1890 Eruption Event & GW150914 GW151226 Passing Events, *2016 EEECOS Conference Proceedings, pp454-457*. http://eeecos.org/conference_proceedings.html

[3] J. Langfellner, L. Gizon, A. C. Birch, Anisotropy of the solar network magnetic field around the average supergranule. *A&A 579, L7 (2015)*. http://lanl.arxiv.org/abs/1505.01427

[4] Ana Cristina Cadavid Cadavid, Yeimy J. Rivera, John K. Lawrence, Damian J. Christian, Peter J. Jennings, A. Franco Rappazzo, Multifractal Solar EUV Intensity Fluctuations and their Implications for Coronal Heating Models. *arXiv:1609.02625v1 (Sep 2016)* http://lanl.arxiv.org/abs/1609.02625

[5] Bogdan Hnat, Sandra C. Chapman, George Rowlands , "Intermittency, scaling and the Fokker-Planck approach to fluctuations of the solar wind bulk plasma parameters as seen by the WIND spacecraft". *Phys. Rev. E, Vol 67, 056404 (2003). arXiv:physics/0211080v2 (2002)*. http://lanl.arxiv.org/abs/physics/0211080

[6] Loukas Vlahos, Theophilos Pisokas, Heinz Isliker, Vassilios Tsiolis, Anastasios Anastasiadis, "Particle Acceleration and Heating by Turbulent Reconnection". *arXiv:1604.05234v4 (2016)*. http://lanl.arxiv.org/abs/1604.05234

[7] Dmitriy Podolskly and Robert Lanza, "On decoherence in quantum gravity", *Annalen der physic, Vol. 528, Issue 9-10, pp663-676 (2016)*. Open Access. http://onlinelibrary.wiley.com/doi/10.1002/andp.201600011/full

[8] Priscilla C. Frisch, Hans-Reinhard Mueller, "Time-variability in the Interstellar Boundary Conditions of the Heliosphere: Effect of the Solar Journey on the Galactic Cosmic Ray Flux at Earth". *arXiv:1010.4507v2 (2010)*. https://arxiv.org/abs/1010.4507

[9] Y. Uprety, M. Chiao, M. R. Collier, T. Cravens, M. Galeazzi, D. Koutroumpa, et al. "Solar Wind Charge Exchange contribution to the ROSAT All Sky Survey Maps". ApJ, Vol 829, 83 (2016). arXiv:1603.03447 (2016). http://lanl.arxiv.org/abs/1603.03447

[10] F. Stefani, A. Giesecke, N. Weber, T. Weier, "Synchronized helicity oscillations: a link between planetary tides and the solar cycle?". *Sol Phys (2016)*, doi:10.1007/s11207-016-0968-0. *arXiv:1511.09335v2 (2016)*. http://lanl.arxiv.org/abs/1511.09335

[11] J. Langfellner, A. C. Birch, L. Gizon," Intensity contrast of the average supergranule", accepted for publication in A&A. *arXiv:1609.09308v1 (Sep 30 2016)*. https://arxiv.org/abs/1609.09308

[12] John Kennewell, Andrew McDonald, "What is a Coronal Hole?" Australian Government Space Weather Services (2015). http://www.sws.bom.gov.au/Educational/2/1/5